



Adaptive Hybrid Control Scheme for Controlling the Position of Coaxial Tri-Rotor UAS

Rana Javed Masood¹, DaoBo Wang¹, Zain Anwar Ali² and Muhammad Anwar²

¹College of Automation Engineering, Nanjing University of Aeronautics and Astronautics, Nanjing, Jiangsu, China.

²Electronic Engineering Department, Sir Syed University of Engineering and Technology, Karachi, Pakistan.

ABSTRACT

In this article, adaptive hybrid control scheme is proposed for controlling the position of a coaxial tri-rotor unmanned aerial system (UAS) in the presence of input saturation and external wind disturbance. The adaptive hybrid controller consists of model reference adaptive control with integral feedback (MRACI) and proportional integral derivative (PID) controller. The adaptive controller deals with the flight dynamics uncertainties and PID controller is used for tuning the gains of MRACI whereas the stability of system is verified by Lyapunov stability criterion. The integrator improves the order of the system thereby improving the convergence rate by rejecting the noise and eliminating steady state errors. Moreover, anti-windup Compensator (AWC) is used to handle the saturation problem. The designed algorithm is applied to a six degree of freedom (6-DOF) nonlinear model of coaxial tri-rotor UAS. Simulations are carried out to validate the reference path of UAS and are compared with MRAC. In this article the wind disturbance test is also performed to check the robustness of the designed controller. It is observed that the proposed algorithm exhibits, quick error convergence, zero steady state error and robustness in the presence of input saturation and external wind disturbance.

KEY WORDS: Position controlling of UAV, adaptive hybrid controller, unmanned aerial system and coaxial tri-rotor.

1 INTRODUCTION

THE control of an Unmanned Aerial System (UAS) has gradually developed a highlighted research field in the robotics society (Portugal, et. al. 2015). Due to its small size, Vertical Take Off and Landing (VTOL) properties, it has the capability of hovering with reduced maintenance and construction (Ortiz, et. al. 2014). Therefore they are widely used in surveillance, monitoring applications like firefighting, agricultural, manholes and armed forces missions (Murphy, et. al. 2016), (Ali, et. al. 2017) and (Yue, et. al. 2012). The aforesaid applications of UAS require perfect control for stability of aerial vehicle that help to work accurately in a hazardous environment.

The research on UAS depends on many areas of engineering like control system, signal communication, aeronautics and astronautics. For study of UAS, many hardware test benches are

required to design the precise aerial vehicle with accurate control structure (Gasior, et. al. 2016). The dynamic model of UAS is highly nonlinear and under-actuated in nature. The classical strategies were previously designed for controlling the nonlinear dynamics of UAS is described in (Ali, et. al. 2016a) and (Pappalardo, et. al. 2017). Additionally, other control algorithms like Proportional Integral Derivative (PID) control (Pounds, et. al. 2012), Nonlinear back-stepping control (Wang, et. al. 2016), Sliding Mode Control, (SMC) (Shima, et. al. 2006) etc., have been designed to control the dynamics of aircraft. In addition, the above-mentioned schemes are used for the stabilization of aerial vehicle provides a trade-off with respect to time. The Model Reference Adaptive Control (MRAC) attract researchers due to its better efficiency for controlling the highly nonlinear dynamics of the system which can vary with respect to time under different internal, external

disturbances and system uncertainties (Shao and Wang 2015). The MRAC algorithm is constructed on behalf of the functions of adaptive switching laws for tracking errors in conjunction with different stability analysis like Massachusetts Institute of Technology (MIT) rule or Lyapunov stability theory which gives the assurance that the trajectory of the aircraft converges at the desired state in finite time (Ghodbane, et. al. 2016). Castillo, O., and Cervantes, L. (2014) have proposed the longitudinal control of the aircraft by augmenting the genetic algorithm which is based on optimal type-1 and type-2 fuzzy systems. The planar vertical takeoff and landing with adjustable pitch propeller rotors for the attitude stabilization of aircraft was proposed by (Lara, et. al. 2014). They give the concept the thrust is induced with the propeller pitch angle instead of varying the speed of rotor and this idea enhances the maneuverability of the aerial vehicle.

To specify the parameters of the controller, stability and its robustness, standard control strategy MRAC is utilized theoretically with the discussion of their structures. For quick convergence of tracking error, the preferred poles of the system are chosen far away from the starting point on the left hand of the system (s-plane) to increase the gain of controller. The MRAC based hybrid control scheme was initially offered by (Hsu, et. al. 2007). The key features of the proposed controller are, to handle the system disturbances, good transient response and robustness of constraint uncertainties. Znidi, et. al. (2016) robust vs MRAC algorithm was designed for quad-rotor aerial vehicle with undefined system dynamics. The adaptive hybrid scheme consists of the fuzzy based Regulation Pole-placement and Tracking (RST) controller by (Ali, et. al. 2016b).

In this paper, MRAC augmented with the proposed adaptive hybrid controller which consists of MRACI and PID scheme for controlling the coaxial tri-rotor UAS. In autonomous systems, MRAC with integral feedback is commonly used such that the adaptive controller is presented to deal with uncertainty in flight dynamics and the gains of MRACI are fine-tuned by the PID controller by (Eugene and Kevin 2013) and (Sarhadi, et. al. 2016). The integrator raises the order of the system and the convergence rate but eliminates the steady state errors and rejects noises. Adaptive control with input saturation and external disturbance is also offered in this article. Model uncertainty and actuator saturation are considered as the main issues to control the autonomous systems. Initially, adaptive control is used to control the model uncertainty in autonomous flight. To handle the input saturation problem, a Riccati based AWC is employed. Furthermore, the wind disturbance test is done to check the robustness of the designed controller. An adaptive hybrid controller shows better efficiency towards the convergence of the system at equilibrium points.

A new methodology is proposed for hybrid control scheme to control the nonlinear dynamics as well as input saturation and external wind disturbance in the UAS. Furthermore, the traditional MRAC method results are not good enough for the convergence of tracking error. As the convergence speed of the nonlinear system is slower than the linear system especially when the adaptable state of the system close to the equilibrium points (Ulrich, et. al. 2012). With the help of a novel adaptive hybrid algorithm, the convergence tracking error of the system proceeds to zero with the definite time of interval. The inspiration of this work is addressed to the difficulty of the desired orientation of UAS, but by utilizing the attractive benefits of adaptive switching laws. This work also points out the problems of robustness, effectiveness, fast error convergence, noises and uncertainties in the model of UAS (Chen, et. al. 2016).

In this paper, adaptive hybrid controller is proposed that has a greater efficiency and better improvement towards the tracking performance in translational and rotational velocity subsystems. Therefore, the most important thing in UAS is its stability time (to change its altitude and the proposed controller quickly to stabilize the system). If the suggested algorithm is failed to stabilize the attitude of the UAS, specifies that the transient performance of the controller is ordinary. For the better transient performance, a new adaptive hybrid algorithm is designed for the dynamic model of coaxial tri-rotor UAS.

The main advancements of this paper are: (1) a new adaptive hybrid controller scheme is designed in which MRACI algorithm removes the system uncertainties and steady state errors, secondly the adaptive gains are regularly fine-tuned by PID controller; (2) the integral action in MRACI helps us to reject the external disturbances; (3) the designed controller uses translational and rotational velocity subsystem, which is most realistic and suitable; (4) stability of the UAS is proven by Lyapunov stability analysis; (5) Riccati-based AWC is used to add the saturation in the system and wind disturbance test is done to check the robustness and efficiency of the control scheme.

The organization of this article is organized as follows. Section 2 defines the coaxial tri-rotor UAS model and its preliminaries followed by the designing of the control structure in section 3. Section 4 demonstrates the simulated results showing the overall robustness, efficiency and validity of the proposed controller. Section 5 concludes the whole article.

2 THE COAXIAL TRI-ROTOR UAS MODEL AND ITS PRELIMINARIES

THIS part of the paper defines the orientation of UAS and its modeling by using the rotational matrix that is followed by the linear and angular velocity

$$\left\{ \begin{array}{l} R_\varphi^x R_\theta^y R_\psi^z = \begin{bmatrix} 1 & 0 & 0 \\ 0 & \cos\varphi & \sin\varphi \\ 0 & -\sin\varphi & \cos\varphi \end{bmatrix} \begin{bmatrix} \cos\theta & 0 & -\sin\theta \\ 0 & 1 & 0 \\ \sin\theta & 0 & \cos\theta \end{bmatrix} \begin{bmatrix} \cos\psi & \sin\psi & 0 \\ -\sin\psi & \cos\psi & 0 \\ 0 & 0 & 1 \end{bmatrix} \\ R_\varphi^x R_\theta^y R_\psi^z = \begin{bmatrix} \cos\theta * \cos\psi & \cos\theta * \sin\psi & -\sin\theta \\ \sin\varphi * \sin\theta * \cos\psi - \cos\psi * \sin\psi & \sin\varphi * \sin\theta * \sin\psi - \cos\varphi * \cos\psi & \sin\varphi * \cos\theta \\ \cos\varphi * \cos\theta * \cos\psi + \sin\varphi * \sin\psi & \cos\varphi * \sin\theta * \sin\psi - \sin\theta * \cos\psi & \cos\psi * \cos\theta \end{bmatrix} \end{array} \right. \quad (1)$$

subsystems of the UAS. The position of the aircraft is demonstrated by using the rotational matrix and it depends upon the Euler angles (Roll, Pitch, Yaw) of the system (Stevens, et. al. 2015). Roll, pitch and yaw (Euler Angles) are used to derive the attitude of the UAS around X, Y, Z axes respectively. Coaxial tri-rotor UAS has six actuators which are fixed in a triangular frame of the aircraft and the system input, output forces and torques is written by,

$$\begin{cases} f_i = kt u_i^2 \rightarrow kt u_i |u_i| \\ \tau_i = k\tau u_i^2 \rightarrow k\tau u_i |u_i| \end{cases} \quad (2)$$

where $i = 1, 2, \dots, 6$ for all six rotors of the UAS.

UAS with coaxial tri-rotor consists of two rotors on each rotational axis having six rotors in a single UAS (Yoo, et. al. 2010). The yaw movement is associated with every axis and is balanced by using rotors having opposite rotation. Therefore it provides greater stability as compared to a single rotor but consumes more power. The core advantage of a tri-rotor UAS over quad-rotor UAS is that it utilizes less power due to three actuators with minimum complexity. All of the above points become major advantages of tri-rotor UAS over quad-rotor UAS (Farooqi, et. al. 2016). For quad-rotor UAS, usually the control problem is to achieve the tracking position of the coordinate system and yaw angle. A common problem exist in tri-rotor is that unpaired rotor reaction produce return torque using yaw angle. The stated problem can be solved easily by placing a servo motor on one of its actuator in a triangular frame of UAS and the tilt angle used to nullify the yaw angle moment. The installation of the servo motor provides one-axis tilt for better movement and sudden turn. The issue stated above of yaw angle from the coaxial tri-rotor point of view can be

resolved by installing two counter rotating actuators to prevent return torque.

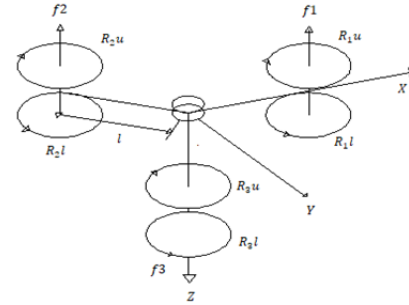


Figure 1. The configuration of the coaxial tri-rotor unmanned aerial vehicle.

Notice that there are two rotors on each rotational axis where the upper one rotates in a clockwise and lower one rotates in an anti-clockwise direction as shown in figure 1 (Yoo, et. al. 2010). It means that both rotors rotate in opposite directions. The main advantage of coaxial rotor is that it does not require any type of motor to avoid yaw moment. Equation (8) and (9) gives force and moment relationship with respect to the model where f_T and τ_T are the total force and turning effect “torque” respectively.

$$\vec{f} = \begin{bmatrix} 0 \\ 0 \\ -(f_{1u} + f_{1l} + f_{2u} + f_{2l} + f_{3u} + f_{3l}) \end{bmatrix} \quad (3)$$

$$\vec{m} = \begin{bmatrix} -(f_{2u} + f_{2l}) * l * \cos(30) + (f_{3u} + f_{3l}) * l * \cos(30) \\ (f_{1u} + f_{1l}) * l - (f_{2u} + f_{2l}) * l * \sin(30) - (f_{3u} + f_{3l}) * l * \sin(30) \\ \tau_{1u} + \tau_{1l} + \tau_{2u} - \tau_{2l} + \tau_{3u} - \tau_{3l} \end{bmatrix} \quad (4)$$

Translational system dynamics are,

$$\begin{cases} \dot{X} = (u_1/m)(\cos\varphi \cos\psi \sin\theta + \sin\psi \sin\varphi) \\ \dot{Y} = (u_1/m)(\sin\theta \sin\psi \cos\varphi - \sin\varphi \cos\psi) \\ \dot{Z} = -g + (u_1/m)(\cos\theta \cos\varphi) \end{cases} \quad (5)$$

Rotational System dynamics are,

$$\begin{cases} \dot{\varphi} = qr(I_y - I_z/I_x) + (l/I_x)u_2 \\ \dot{\theta} = pr(I_z - I_x/I_y) + (l/I_y)u_3 \\ \dot{\psi} = pq(I_x - I_y/I_z) + (l/I_z)u_4 \end{cases} \quad (6)$$

The (u, v, w) and (p, q, r) are the linear and angular velocities of UAS, g is the center of gravity; m is mass and l is the distance from the center towards the rotor of the UAS (Mederreg, et. al. 2003). To derive the model of the UAV by using its rotational subsystem

and input of all the rotors which are used in (Das, et. al, 2009), the input state space vector is written as “X”, controller and output vector is written as “ $U_S(t)$ ” and “ $Y_S(t)$ ”.

$$\begin{cases} \dot{X}_S(t) = f(X_S(t), U_S(t)) \\ Y_S(t) = h(X_S(t)) \end{cases} \quad (7)$$

Following are the state space models,

$$\begin{cases} \dot{X}_S(t) = [p, q, r, u_1, u_2, u_3, u_4] \\ U_S(t) = [u_1, u_2, u_3, u_4] \\ Y_S(t) = [p, q, r] \end{cases} \quad (8)$$

The electric motors may take as input to linearize physical model which indicates the rotation rates of UAV. Now steady state solution can help to linearize the nonlinear behavior of the system, which correspond to zero and then it provides equilibrium of the system. Simply UAV should be linearized around the equilibrium points $X'_{So}(t)$, $U'_{So}(t)$.

$$f(X'_{So}(t), U'_{So}(t)) \equiv 0 \quad (9)$$

Trim point conditions are used to linearize the system it means that the operating point of the UAV is specified by the input torque on the rotors of the vehicle.

$$\begin{cases} A_{m,n} = \frac{\delta f_m(X'_{So}(t), U'_{So}(t))}{\delta X_n} \\ B_{m,n} = \frac{\delta f_m(X'_{So}(t), U'_{So}(t))}{\delta U_n} \\ C_{m,n} = \frac{\delta h_m(X'_{So}(t))}{\delta X_n} \end{cases} \quad (10)$$

Four constants $B_{4,1}$, $B_{5,2}$, $B_{6,3}$ & $B_{7,4}$ and equation (12) represents the linear system matrix. The angular velocity components (physical model) shown in the equation (06).

To linearize the nonlinear equations by using the equation (10),

$$\begin{cases} A_{1,5} = \frac{\delta \dot{p}}{\delta u_2} = (1/I_x)(\sqrt{3} * l * kt * u_2) \\ A_{1,6} = \frac{\delta \dot{p}}{\delta u_3} = (-1/I_y)(\sqrt{3} * l * kt * u_3) \\ A_{2,4} = \frac{\delta \dot{q}}{\delta u_1} = \left(\frac{1}{I_y}\right)(2 * u_1)(kt * \sin u_4 - l * kt * \cos u_4) \\ A_{2,5} = \frac{\delta \dot{q}}{\delta u_2} = \left(\frac{1}{I_y}\right)(l * kt * u_2) \\ A_{2,6} = \frac{\delta \dot{q}}{\delta u_3} = \left(\frac{1}{I_y}\right)(l * kt * u_3) \\ A_{2,7} = \frac{\delta \dot{q}}{\delta u_4} = \left(\frac{1}{I_y}\right)(u_1 |u_1|)(kt * \sin u_4 + kt * \cos u_4) \\ A_{3,4} = \frac{\delta \dot{r}}{\delta u_1} = \left(-\frac{1}{I_z}\right)(2 * u_1)(l * kt * \sin u_4 + kt * \cos u_4) \\ A_{3,5} = \frac{\delta \dot{r}}{\delta u_2} = \left(-\frac{1}{I_z}\right)(2 * kt * u_2) \\ A_{3,6} = \frac{\delta \dot{r}}{\delta u_3} = \left(-\frac{1}{I_z}\right)(2 * kt * u_3) \\ A_{3,7} = \frac{\delta \dot{r}}{\delta u_4} = \left(\frac{1}{I_z}\right)(u_1 |u_1|)(kt * \sin u_4 - l * kt * \cos u_4) \end{cases} \quad (11)$$

$$\begin{cases} A_S = \begin{bmatrix} -10^{-11} & 0 & 0 & 0 & A_{1,5} & A_{1,6} & 0 \\ 0 & -10^{-11} & 0 & A_{2,4} & A_{2,5} & A_{2,6} & A_{2,7} \\ 0 & 0 & -10^{-11} & A_{3,4} & A_{3,5} & A_{3,6} & A_{3,7} \\ 0 & 0 & 0 & A_{4,4} & 0 & 0 & 0 \\ 0 & 0 & 0 & 0 & A_{5,5} & 0 & 0 \\ 0 & 0 & 0 & 0 & 0 & A_{6,6} & 0 \\ 0 & 0 & 0 & 0 & 0 & 0 & 0 \end{bmatrix} \\ B_S = \begin{bmatrix} 0 & 0 & 0 & 0 & 0 \\ 0 & 0 & 0 & 0 & 0 \\ 0 & 0 & 0 & 0 & 0 \\ B_{4,1} & 0 & 0 & 0 & 0 \\ 0 & B_{5,2} & 0 & 0 & 0 \\ 0 & 0 & B_{6,3} & 0 & 0 \\ 0 & 0 & 0 & B_{7,4} & 0 \end{bmatrix} \\ C_S = \begin{bmatrix} 1 & 0 & 0 & 0 & 0 & 0 & 0 \\ 0 & 1 & 0 & 0 & 0 & 0 & 0 \\ 0 & 0 & 1 & 0 & 0 & 0 & 0 \end{bmatrix} \end{cases} \quad (12)$$

Table 1. UAS constants and its dynamics.

No.	Reference Frame	Euler Angles and Orientation	Translational and Rotational Velocities	Forces and Inertial Moments
1	Movement along the x axis	x	u	X
2	Movement along the y axis	y	v	Y
3	Movement along the z axis	z	w	Z
4	Rotation at x axis Roll	φ	p	lx
5	Rotation at y axis Pitch	θ	q	ly
6	Rotation at z axis Yaw	ψ	r	lz

The orientation of UAS is moderate by using Euler angles which has a command to control the altitude as well as the attitude that rotates at global axis (Phillips, et. al. 2001). Furthermore, the global axis system, force components, linear velocities, angular velocities and inertial system constants are defined in Table 1.

3 DESIGNING OF CONTROL ARCHITECTURE

THE control architecture of coaxial tri-rotor UAS is same as that of the single rotor UAS. Moreover, the control strategies and designing of controller is not same as simple tri-rotor UAS.

3.1 Control Strategies

All the control strategies of the aircraft is described below in which the speed of rotors are denoted by “ δ ” (Yoo, et. al. 2010).

Altitude Control. Control the height of the UAS. The all six rotors must be control (speed) simultaneously which is responsible for the altitude variations of the UAS. Mathematically, states that $\delta 1_u = \delta 1_l = \delta 2_u = \delta 2_l = \delta 3_u = \delta 3_l$.

Roll and Pitch Control. The roll and pitch moments are controlled by increasing the tail rotor speed of both (upper and lower) rotors which lead to a rolling moment and vice-versa. Rolling controls the pitch of the tri-rotor. Mathematically, shows that (for nose-down) $\delta 2_u = \delta 2_l = \delta 3_u = \delta 3_l < \delta 1_u = \delta 1_l$, for (nose-up) $\delta 1_u = \delta 1_l > \delta 2_u = \delta 2_l = \delta 3_u = \delta 3_l$.

Yaw Control. The variation in the lower and upper rotors may be used to control the yaw by producing a torque, which definitely control the yaw moment of UAS. Mathematically, shows that (clockwise) $\delta 1_u = \delta 2_u = \delta 3_u > \delta 1_l = \delta 2_l = \delta 3_l$, for (anticlockwise) $\delta 1_l = \delta 2_l = \delta 3_l > \delta 1_u = \delta 2_u = \delta 3_u$.

3.2 Adaptive hybrid algorithm.

Model reference adaptive control with integral feedback is mostly used in autonomous systems like UAS, AUV (Autonomous Underwater Vehicles) etc. (Eugene and Kevin, 2013) and (Sarhadi, et. al. 2016). The characteristic of this algorithm is to build up a response by an integral state in which its gains are frequently adjusted by the PID controller, which is also termed as an adaptive hybrid controller. The process of an amplified adaptation with approaching technique with the system uncertainties in the dynamics of the autonomous structure. In the meantime, integral state feedback is responsible for the cancellation of the noise (Hu, et. al. 2016). Figure 2 defines the complete structure of our designed controller.

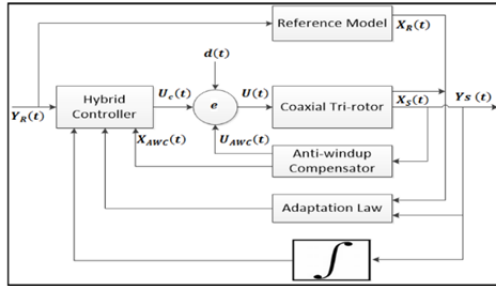


Figure 2. Control Structure of the hybrid controller with Integral feedback.

The above controller design is based on the controlling the position of the coaxial UAV with wind disturbance $d(t)$.

$$\begin{cases} \dot{X}_s(t) = A_s X_s(t) + B_s \gamma(U(t)) + d(t) \\ Y_s(t) = C_s X_s(t) \end{cases} \quad (13)$$

where the complete system representation is depending on time, $X_s(t)$ State variables of the system, $Y_s(t)$ output of the system, $U(t)$ control input, A_s, B_s, C_s are system matrices, $\gamma \in R^{m \times m}$ constant diagonal unknown matrix, and $d(t)$ external disturbance. Now the tracking error of the entire system with respect to integral feedback can be written as,

$$e_I(t) = \int_0^t Y_s(t) - Y_R(t) \quad (14)$$

where $Y_s(t)$ is the system actual and $Y_R(t)$ is the reference output's state of the system with respect to time due to its varying ability. The controller major topic is to force $Y_s(t)$ to follow the output reference signal $Y_R(t)$ in which controller major task is to force the actual system to follow the reference system and can be regulated. By augmented the state vector, $X(t) = [e_I^T(t) C_s e_I(t)]^T$. Now the open-loop generalize form of equation (13) is written as,

$$\begin{cases} \dot{X}(t) = AX(t) + B\gamma(U(t)) + B_R Y_R(t) \\ Y(t) = CX(t) \end{cases} \quad (15)$$

where, the extended form of system matrix is $X(t) = (e_I^T(t) X_s^T(t))^T$ and their dimension is written as, $n = n_s + m$. The extended open loop matrices is written as,

$$\begin{aligned} A &= \begin{bmatrix} 0 & C_s \\ 0 & A_s \end{bmatrix}; B = \begin{bmatrix} 0 \\ B_s \end{bmatrix}; \\ Y_s(t) &= [0 \ C_s]; B_s = \begin{bmatrix} -1 \end{bmatrix} \end{aligned} \quad (16)$$

The controllability of extended pair matrices is shown in (16) which is $(A, (B \gamma))$. It is not hard to appear the extended pair is controllable when; $\det \begin{pmatrix} A_s & B_s \gamma \\ C_s & 0 \end{pmatrix} \neq 0$. The most important need of suggested controller is to follow the output of the system $Y_s(t)$ and time varying reference signal $Y_R(t)$ in the occurrence of uncertain system dynamics of A and γ . The Hurwitz matrix can be considered as a reference A_R connected with an unknown constant and positive diagonal of γ . At present, the output of the required system can be established by this matrix.

$$A_R = A + B\gamma\rho_X^T \quad (17)$$

Equation (17) provides the matching condition of the system. Now by substituting (17) into equation (15) gives,

$$\dot{X}(t) = A_R X(t) + B\gamma(U_c(t) - \rho_X^T X(t)) + B_R Y_R(t) \quad (18)$$

A predictable control scheme is proposed in which MRACI and PID is combined. For this proposed algorithm, the control signal $U(t)$ in (15) is built for the combination of two inputs.

$$U(t) = U_{MRACI}(t) + U_{PID}(t) \quad (19)$$

The different roles of two inputs are as follows,

$$\begin{cases} U_{MRACI}(t) = \hat{\rho}_x^T(X_s(t)) \\ U_{PID}(t) = k_{PID}X = -k_p e_f(t) - k_i \int_0^t e_f(t) - \\ k_d(e_f(t)d/dt) \end{cases} \quad (20)$$

The goal of the PID controller is to generalize the poles of a closed loop system in a mode in which reference system matrix A_R is attained and have information about A and γ matrix. In the present uncertainties model of the system, the usually PID controller is not able to follow the preferred output of the UAS. Therefore, the hybrid controller is proposed in this study to track the desired or reference path of the UAS. Currently the algorithm of the anticipated controller for the UAS, the most accurate system matrices are less known. Therefore, the MRACI takes part to deal with uncertainties substituting the adaptive controller part U_{MRACI} in the equation (18).

$$\dot{X}(t) = A_R X(t) + B\gamma(\rho_x^T X) + B_R Y_R(t) \quad (21)$$

The reference system on behalf of (21) is written by,

$$\dot{X}_R(t) = A_R X_R(t) + B_R Y_R(t) \quad (22)$$

Now, the state error tracking could be,

$$e(t) = X(t) - X_R(t) \quad (23)$$

The dynamics of the error is defined as,

$$\dot{e}(t) = A_R e(t) + B\gamma(\rho_x^T X) \quad (24)$$

Theorem: By using Lyapunov candidate function, the convergence of the system error signal can be written as,

$$\dot{v}(e(t)) = e^T(t)P_R e(t) + \text{trace}(\Delta\rho_x^T \beta_x^{-1} \gamma \Delta\rho_x) \quad (25)$$

Proof: β_x is the adaptation rate and $\text{trace}(\cdot)$ is the operator of matrix trace, the diagonal matrix $P_R = P_R^T > 0$, now by neglecting the other variants to classify the resolution of Lyapunov candidate task that is $A_R^T P_R + P_R A_R = -Q$. The positive specific matrix which would be written as $Q = Q^T > 0$. The derivative of Lyapunov candidate function is as follows,

$$\begin{aligned} \dot{v}(e(t)) = & -e^T(t)Qe(t) \\ & + 2\text{trace}(\Delta\rho_x^T \{\beta_x^{-1} \hat{\rho}_x \\ & + Xe^T(t)BP\}\gamma) \end{aligned} \quad (26)$$

Therefore, by applying “trace” as a vector identity which is valid for only two dimensional vectors A & B can be written as, $A^T B = \text{trace}(BA^T)$ and adaptive law can be written as,

$$\dot{\hat{\rho}}_x = -\beta_x X e^T(t)BP. \quad (27)$$

Then the resultant is,

$$\dot{v}(e(t)) = -e^T(t)Qe(t) \leq 0 \quad (28)$$

Which confirms the desired stability of the system.

3.3 Anti-windup compensator with wind disturbance test.

The proposed adaptive hybrid controllers have their own constructive feature in the model. However, the uncertainties of the system can deal with the adaptive controller in which integral action can help the system to remove the disturbances in the system. Moreover, the Anti-Windup Compensator (AWC) is used to adjust the performance of the controller when the input saturation in the UAV dynamics occurs (Turner, et. al. 2015). Lastly, the efficiency of the system is cross checked by adding the continuous wind disturbance in the system to ensure the robustness and efficiency of the controller. Now, by considering the Riccati based controllable and Observable equation (Kahveci, 2009) which can be written as,

$$A_{AWC}^T P + PA_{AWC} + Q - PB_{AWC}R^{-1}B_{AWC}^T P = 0 \quad (29)$$

Where, it could be shown in state-space representation now the entire system can be written as,

$$\begin{aligned} A_{AWC} &= A + BLQ^{-1}, B_{AWC} = B, \\ C_{AWC} &= [(LQ^{-1})^T I]^T, D_{AWC} = 0 \end{aligned} \quad (30)$$

By implementing LQ^{-1} for anti-windup compensator matrices, A_{AWC} and C_{AWC} where $A + BLQ^{-1}$, is Hurwitz and $Q > 0$ and $U > 0$. The AWC can be described as,

$$\dot{X}_{AWC}(t) = A_{AWC}X_{AWC}(t) + B_{AWC}U_{AWC}(t) \quad (31)$$

The $U_{AWC}(t)$ and $X_{AWC}(t)$ are the controller and input of AWC. The saturation of the system can be calculated as,

$$U_{AWC}(t) = \text{sat}\{\text{sgn}(U_c(t))\}, \quad (32)$$

where

$$\text{sgn}(U_c(t)) = \begin{cases} 1 & \text{for } U_c(t) > 0 \\ 0 & \text{for } U_c(t) = 0 \\ -1 & \text{for } U_c(t) < 0 \end{cases} \quad (33)$$

The modified control signal could be,

$$U_c(t) = k_{PID}(X(t) + X_{AWC}(t)) + \hat{\rho}_x^T(X(t) + X_{AWC}(t)) - U_{AWC}(t) \quad (34)$$

(Wind disturbance test): Initially, wind disturbance is in the direction as that of flight, thus causes the flight to deviate from the reference path, and in certain circumstances, this may lead to flight failure. Therefore, in this study, wind disturbance test is included to validate the proposed adaptive hybrid controller. In order to perform the test, artificial wind is created (Venugopalan, et. al. 2012), as described by the wind velocity polynomial

$$W_V = -1.13x^5 + 4.35x^4 - .629x^3 + 3.49x^2 - 2.79x + 3.19 \quad (35)$$

The controller efficiency is validated by taking the wind velocity from the UAV's x-axis i-e 1.25m/sec, causing 12.5° change in roll angle to hovering state. Since, the gravity " g_e " is supposed to be equal to the hovering state " u_x ", therefore the wind disturbance is applied to roll angle along UAV's x-axis.

$$u_x = \frac{g_e}{\tan\phi} \quad (36)$$

Moreover, tri-rotor UAV's are appearing to be slow for any change in aerodynamic interface, noise or wind disturbances, therefore a constraint in wind disturbance is incorporated as follows

$$\begin{cases} \bar{u}_x = u_x \sin(4\pi t) + d_{F1} + \tilde{A}.rands() \\ \bar{u}_y = u_y \cos(2 = 4\pi t) + d_{F2} + \tilde{A}.rands() \\ \bar{u}_z = d_{F3} + \tilde{A}.rands() \end{cases} \quad (37)$$

where the wind disturbance external forces are written as, " \bar{u}_x ", " \bar{u}_y " and " \bar{u}_z " beside with the nonlinearity applied to the aerial vehicle in the direction of universal axes respectively, whereas the constant components of wind are " u_x " and " u_y ". The degree of random noise is denoted as " \tilde{A} " and the varying time interface force is written as; $d(t) = [d_{F1}, d_{F2}, d_{F3}]$. Now rewrite the aerodynamic interface force which is,

$$d(t) = \begin{bmatrix} 0.1\sin(0.1\pi t), 0.1\cos(0.1\pi t), \\ 0.1\cos(0.1\pi t) \end{bmatrix} \quad (38)$$

3.4 Simulation Results and Discussions.

In this section, the simulated results to verify the effectiveness and validity of the proposed control algorithm. The control diagram of the proposed controller is shown in figure 2 and control algorithm is simulated on Simulink MATLAB for the validation. The model constraints and controller constraints of the UAS are defined in table 2 and 3 respectively.

The selected state for hovering of UAS uses input as a reference signal which is constant and the orientation of the system is fixed by stabilizing its attitude angles. The variable input of the system used as a reference state with the help of linear and angular velocities of the UAS that appears to be real presentation. The effectiveness of the proposed controller is proven and shown in the results of the

reference state. Furthermore, translational and rotational velocity subsystems help UAS to reach the reference state. Whereas, the primarily error is measured by angular velocity subsystem to reach the preferred location of the UAS at the desired position. The complete performance of the UAS is governed by MRACI, its gains are fine-tuned by PID controller and stability is proved by Lyapunov stability function. Simulations in figure 03-07 show the robustness and effectiveness of the proposed controller.

Table 2. Model and controller constraints of UAS

Constraints	Standards	S.I Units
(Mass) "m"	1.482	Kg
(G.F) "g"	9.81	m/s2
l	0.4252	m
l_x	0.4015	Kgm2
l_y	0.4015	Kgm2
l_z	0.4221	Kgm2
u_x	0.75	N
u_y	0.75	N
\tilde{A}	0.19	-
ρ	0.015	-

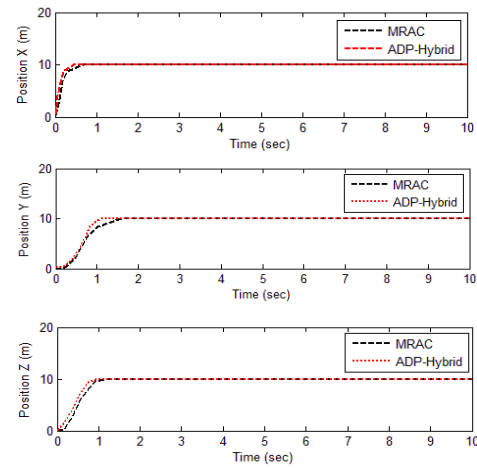


Figure 3(a), (b), (c). The Orientation of the UAS.

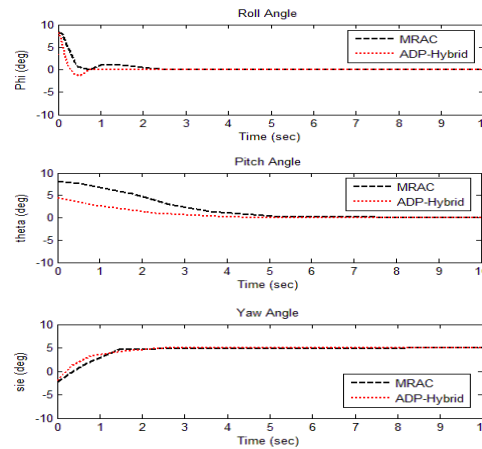


Figure 4(a), (b), (c). The Euler angles of the UAS.

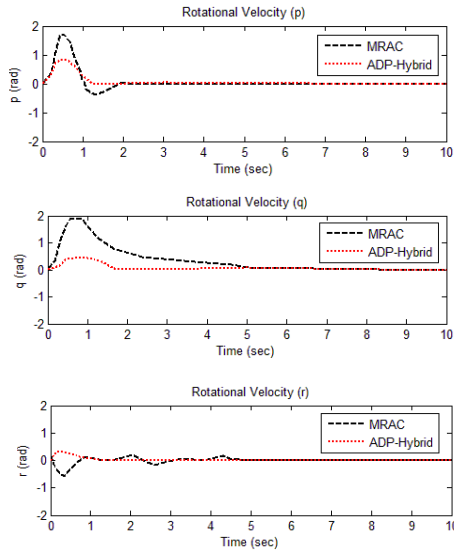


Figure 5(a), (b), (c). The Rotational Velocities of the UAS.

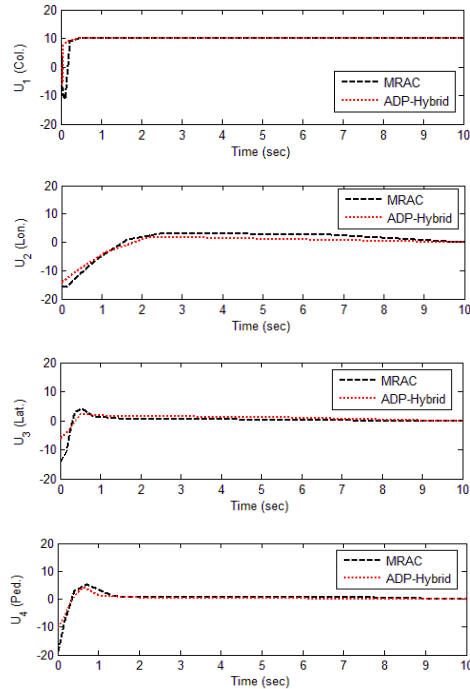


Figure 07(a), (b), (c), (d). The Control Input of the UAS.

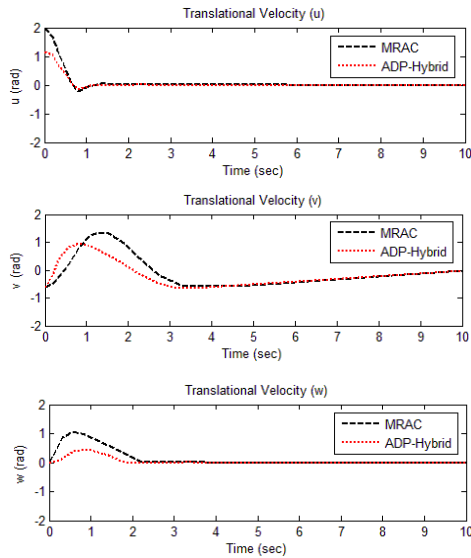


Figure 06(a), (b), (c). The Translational Velocities of the UAS.

The starting position of the UAS in this case is (0, 0, 0) m and (9, 9, -2) deg whereas the desired position and attitude angles are: $x=y=z=10$ m, $\varphi=\theta=0$ and $\psi=5$ deg shown in figures 03(a), (b), (c) and 04(a), (b), (c) respectively. The designed scheme of the UAV managed to control the coaxial tri-rotor at the preferred altitude and attitude in a short interval of time. The elevation z and yaw angle Ψ noticeably shows that it converges to the desired response rapidly without any oscillations. Furthermore, the altitude z reaches to the preferred value at u_1 . The roll and pitch angles have small oscillations to reach the preferred value but there is very little variation in their amplitude.

The angular and linear velocities are shown in figure 05 and 06 respectively showing the same response as the conforming location and attitude angle. These velocity responses represent the robustness and validity of the proposed controller.

Input (u_1, u_2, u_3, u_4) responses shown in figure 07 demonstrate the input controller converges to their desired values at (10, 0, 0, and 0) after a very short interval of time. However, $u_1 \neq 0$ confirms the time invariant in a finite interval of time. Moreover, initial responses of u_1 and u_4 have high fluctuations in their amplitude. The aerodynamics forces have uncertainty problems which are taken as a disturbance in the model of coaxial tri-rotor UAV.

The disturbances of the proposed controller are not visible which may lead to designing phase. Therefore, two computer simulations are implemented to check the validity of the designed hybrid controller scheme which is based on its altitude and position tracking of the UAS. After that it will clearly see that the controller converges to the desired value in a short interval of a time, but their convergence rate is apparently dissimilar. The results show that the designed controller is reliable and have fast convergence at desired values with no steady state error to perform the altitude and attitude tracking of coaxial tri-rotor UAS.

4 CONCLUSION

THIS article proposes adaptive hybrid controller for controlling the position of coaxial UAS in the presence of input saturation and external wind

disturbance. The AWC controlled the input saturation significantly in the presence of wind disturbance. The designed scheme stabilized the dynamic uncertainty with greater potential to the actuators of the UAS. The proposed controller handled the input saturation, model uncertainty and wind disturbance effectively. Moreover, the controller validates the desired or reference path of UAS. The performance of our proposed hybrid controller outperforms all previous MRAC based control schemes.

5 ACKNOWLEDGMENT

THIS work was supported by the key laboratory of (S&mc) lab College of Automation Engineering, Nanjing University of Aeronautics and Astronautics, Nanjing, China.

6 REFERENCES

- Z. A. Ali, D. B. Wang, and M. S. Loya. (2017). SURF and LA with RGB Vector Space Based Detection and Monitoring of Manholes with an Application to Tri-Rotor UAS Images. *International Journal of Engineering and Technology*, 9(1), 32.
- Z. A. Ali, D. Wang, and M. Aamir. (2016b). Fuzzy-Based hybrid control algorithm for the stabilization of a tri-rotor UAV. *Sensors*, 16(5), 652.
- Z. A. Ali, D. Wang, S. Masroor, and M. S. Loya. (2016a). Attitude and Altitude Control of Trirotor UAV by Using Adaptive Hybrid Controller. *Journal of Control Science and Engineering*, 2016.
- O. Castillo and L. Cervantes. (2014). Genetic design of optimal type-1 and type-2 fuzzy systems for longitudinal control of an airplane. *Intelligent Automation and Soft Computing*, 20(2), 213-227.
- C.-S. Chen and W.-L. Chen. "Robust adaptive sliding-mode control using fuzzy modeling for an inverted-pendulum system." *IEEE Transactions on Industrial Electronics* 45, no. 2 (1998): 297-306.
- F. Chen, R. Jiang, K. Zhang, B. Jiang, and G. Tao. (2016). Robust backstepping sliding-mode control and observer-based fault estimation for a quadrotor UAV. *IEEE Transactions on Industrial Electronics*, 63(8), 5044-5056.
- A. Das, F. Lewis, and K. Subbarao. (2009). Backstepping approach for controlling a quadrotor using lagrange form dynamics. *Journal of Intelligent and Robotic Systems*, 56(1-2), 127-151.
- L. Eugene and W. Kevin. (2013). Robust and adaptive control with aerospace applications.
- M. A. A. Farooqi, F. M. Malik, J. Anwar, and M. Ali. (2016). Sampled Data Output Feedback Control of Tri Rotor Unmanned Aerial Vehicle. *Science International*, 28(1).
- P. Gasior, A. Bondyra, S. Gardecki, W. Giernacki, and A. Kasiński. (2016). Thrust estimation by fuzzy modeling of coaxial propulsion unit for multirotor UAVs. In *Multisensor Fusion and Integration for Intelligent Systems (MFI)*, 2016 IEEE International Conference on (pp. 418-423). IEEE.
- A. Ghodbane, M. Saad, C. Hobeika, J. F. Boland, and C. Thibeault. (2016). Design of a tolerant flight control system in response to multiple actuator control signal faults induced by cosmic rays. *IEEE Transactions on Aerospace and Electronic Systems*, 52(2), 681-697.
- L. Hsu, R. R. Costa, and F. Lizarralde. (2007). Lyapunov/passivity-based adaptive control of relative degree two MIMO systems with an application to visual servoing. *IEEE Transactions on Automatic Control*, 52(2), 364-371.
- J. Hu, Y. Qiu, and L. Liu. (2016). High-order sliding-mode observer based output feedback adaptive robust control of a launching platform with backstepping. *International Journal of Control*, 89(10), 2029-2039.
- N. E. Kahveci, (2009). Adaptive Control Design for Uncertain and Constrained Vehicle Yaw Dynamics. In *Frontiers in Adaptive Control*. InTech.
- D. Lara, M. Panduro, G. Romero, E. Alcorta, and R. Betancourt. (2014). Robust control design techniques using differential evolution algorithms applied to the pvtol. *Intelligent Automation and Soft Computing*, 20(3), 451-466.
- L. Mederreg, F. Diaz, and N. K. M'sirdi. (2003). Nonlinear backstepping control with observer design for a 4 rotors helicopter. *AVCS*, 4, 28-31.
- R. R. Murphy, S. Tadokoro, and A. Kleiner. (2016). Disaster Robotics. In *Springer Handbook of Robotics* (pp. 1577-1604). Springer International Publishing.
- A. Ortiz, F. Bonnin-Pascual, and E. Garcia-Fidalgo. (2014). Vessel inspection: A micro-aerial vehicle-based approach. *Journal of Intelligent and Robotic Systems*, 76(1), 151-167.
- C. M. Pappalardo and D. Guida. (2017). Adjoint-based optimization procedure for active vibration control of nonlinear mechanical systems. *Journal of Dynamic Systems, Measurement, and Control*, 139(8), 081010.
- W. F. Phillips, C. E. Hailey, and G. A. Gebert. (2001). Review of attitude representations used for aircraft kinematics. *Journal of aircraft*, 38(4), 718-737.
- D. Portugal, G. Cabrita, D. B. Gouveia, D. C. Santos, and J. A. Prado. (2015). An autonomous all terrain robotic system for field demining missions. *Robotics and Autonomous Systems*, 70(C), 126-144.
- P. E. Pounds, D. R. Bersak, and A. M. Dollar. (2012). Stability of small-scale UAV helicopters and quadrotors with added payload mass under PID control. *Autonomous Robots*, 33(1-2), 129-142.
- P. Sarhadi, A. R. Noei, and A. Khosravi. (2016). Model reference adaptive PID control with anti-windup compensator for an autonomous

underwater vehicle. *Robotics and Autonomous Systems*, 83, 87-93.

- X. Shao and H. Wang. (2015). Active disturbance rejection based trajectory linearization control for hypersonic reentry vehicle with bounded uncertainties. *ISA transactions*, 54, 27-38.
- T. Shima, M. Idan, and O. M. Golan. (2006). Sliding-mode control for integrated missile autopilot guidance. *Journal of guidance, control, and dynamics*, 29(2), 250-260.
- B. L. Stevens, F. L. Lewis, and E. N. Johnson. (2015). *Aircraft control and simulation: dynamics, controls design, and autonomous systems*. John Wiley and Sons.
- M. C. Turner and R. T. O'Brien. (2015). An anti-windup scheme for an adaptive \mathcal{H}_∞ vibration controller: Development and simulations. In *American Control Conference (ACC)*, 2015 (pp. 5306-5311). IEEE.
- S. Ulrich, J. Z. Sasiadek and I. Barkana. (2012). Modeling and direct adaptive control of a flexible-joint manipulator. *Journal of Guidance, Control and Dynamics*, 35(1), 25-39.
- T. K. Venugopalan, T. Taher, and G. Barbastathis. (2012). Autonomous landing of an Unmanned Aerial Vehicle on an autonomous marine vehicle. In *Oceans*, 2012 (pp. 1-9). IEEE.
- D. B. Wang, Z. A. Ali, and M. Aamir. (2016). Hybrid Strategy for Nonlinear Control of (6 DOF) Under Actuated Tricolor UAV. *International Journal of Control and Automation*, 9(12), 463-472.
- D. W. Yoo, H. D. Oh, D. Y. Won, and M. J. Tahk. (2010, June). Dynamic modeling and control system design for Tri-Rotor UAV. In *Systems and Control in Aeronautics and Astronautics (ISSCAA)*, 2010 3rd International Symposium on (pp. 762-767). IEEE.
- J. Yue, T. Lei, C. Li, and J. Zhu. (2012). The application of unmanned aerial vehicle remote sensing in quickly monitoring crop pests. *Intelligent Automation and Soft Computing*, 18(8), 1043-1052.
- A. Znidi, K. Dehri, and A. S. Nouri. (2016). Discrete variable structure model reference adaptive control using only input-output measurements. *Transactions of the Institute of Measurement and Control*, 0142331216668392.

7 DISCLOSURE STATEMENT

NO potential conflict of interest was reported by the authors.

8 NOTES OF CONTRIBUTORS



Rana Javed Masood, has received the Masters of Engineering in the field of Industrial Control and Automation from Hamdard University of Engineering and Technology Karachi, Pakistan and is currently a Ph.D. research Scholar in the field of Control theory and Control Engineering at College of Automation Engineering, Nanjing University of Aeronautics and Astronautics, China. Current research interest focuses on the Virtual Reference Feedback Tuning, Data Driven Control, MFA Control, Servo based turntable and motion simulation Control.



Dao Bo Wang, Professor in the College of Automation Engineering at Nanjing University of Aeronautics and Astronautics, China. He was an official designated visiting scholar at the University of Bath, UK from 1987 to 1989 and senior visiting scholar at the University of Waterloo, Ontario, Canada in 1999. His research interests include Unmanned Aerial Vehicle Flight Control, Servo and Hydraulic based Turn Tables and Motion Simulators.
Email: dbwangpe@nuaa.edu.cn



Zain Anwar Ali, received the B.S. degree in electronic engineering from the Sir Syed University of Engineering and Technology, Karachi, Pakistan in 2010. He did PhD in control theory and control engineering from Nanjing University of Aeronautics and Astronautics, Nanjing, China. He is working as an Assistant Professor in the Department of Electronic Engineering, SSUET, Karachi, Pakistan.
Email: zainanwar86@hotmail.com



Muhammad Anwar Ahmed, has received the Masters of Engineering in the field of Industrial electronics from Sir Syed University of Engineering and Technology Karachi, Pakistan. He is the faculty member in electronic engineering department since 2013. Current research interest focuses on the industrial automation, control theory and optoelectronics.
Email: enr_anwar_ahmed@outlook.com